Iron as a source of efficient Shockley-Read-Hall recombination in GaN

Darshana Wickramaratne, Jimmy-Xuan Shen, Cyrus E. Dreyer, Manuel Engel, Martijn Marsman, Georg Kresse, Saulius Marcinkevičius, Audrius Alkauskas, and Chris G. Van de Walle

Citation: Applied Physics Letters **109**, 162107 (2016); doi: 10.1063/1.4964831
View online: http://dx.doi.org/10.1063/1.4964831
View Table of Contents: http://scitation.aip.org/content/aip/journal/apl/109/16?ver=pdfcov
Published by the AIP Publishing

Iron as a source of efficient Shockley-Read-Hall recombination in GaN

Darshana Wickramaratne,[1] Jimmy-Xuan Shen,[2] Cyrus E. Dreyer,[1,3] Manuel Engel,[4] Martijn Marsman,[4] Georg Kresse,[4] Saulius Marcinkevičius,[5] Audrius Alkauskas,[6] and Chris G. Van de Walle[1]

[1]*Materials Department, University of California, Santa Barbara, California 93106-5050, USA*
[2]*Department of Physics, University of California, Santa Barbara, California 93106-9530, USA*
[3]*Department of Physics and Astronomy, Rutgers University, Piscataway, New Jersey 08845-0849, USA*
[4]*Faculty of Physics, Computational Materials Physics, University of Vienna, Vienna A-1090, Austria*
[5]*Department of Materials and Nano Physics, KTH Royal Institute of Technology, Electrum 229, 16440 Kista, Sweden*
[6]*Center for Physical Sciences and Technology, Vilnius LT-10257, Lithuania*

(Received 15 July 2016; accepted 1 October 2016; published online 21 October 2016)

Transition metal impurities are known to adversely affect the efficiency of electronic and optoelectronic devices by introducing midgap defect levels that can act as efficient Shockley-Read-Hall centers. Iron impurities in GaN do not follow this pattern: their defect level is close to the conduction band and hence far from midgap. Using hybrid functional first-principles calculations, we uncover the electronic properties of Fe and we demonstrate that its high efficiency as a nonradiative center is due to a recombination cycle involving excited states. Unintentional incorporation of iron impurities at modest concentrations ($10^{15}\,cm^{-3}$) leads to nanosecond nonradiative recombination lifetimes, which can be detrimental for the efficiency of electronic and optoelectronic devices. *Published by AIP Publishing.* [http://dx.doi.org/10.1063/1.4964831]

The Group-III nitride semiconductors and their alloys are being investigated for a wide variety of commercial applications. They are the active material in light-emitting diodes,[1] in high electron mobility transistors (HEMTs),[2] and in tunnel devices.[3] Fabrication of electronic devices requires the use of semi-insulating substrates or buffer layers, and Fe is used as an acceptor that compensates the unintentional *n*-type GaN.[4] Research on Fe in GaN has also been motivated by efforts to achieve room-temperature ferromagnetism in GaN.[5] In addition, unintentional incorporation of iron during epitaxial growth of GaN can be due to memory effects, or result from the presence of silica or alumina components in the system, or from the reaction of amides and halides formed from gas sources with stainless steel components.[6]

Transition-metal impurities in semiconductors tend to form defect levels deep in the bandgap; for instance, copper, iron, or gold in silicon lead to multiple levels within the gap.[7] These levels enable efficient Shockley-Read-Hall (SRH) recombination, as evidenced by large capture cross sections ($\sim 10^{-15}\,cm^2$).[7] The SRH recombination has been blamed for efficiency losses in optoelectronic[8] and electronic devices.[9] For a defect density N and electron (hole) capture coefficients C_n (C_p), the SRH recombination coefficient A is defined as[10,11]

$$A = N\frac{C_n C_p}{C_n + C_p}. \quad (1)$$

There are strong experimental indications that Fe in GaN acts as an efficient nonradiative center. Using time-resolved photoluminescence,[12,13] electron and hole capture coefficients $C_n = 5.5 \times 10^{-8}\ cm^3\ s^{-1}$ and $C_p = 1.8 \times 10^{-8}\ cm^3\ s^{-1}$ have been obtained for GaN samples intentionally doped with Fe. Such large capture coefficients indicate that a low concentration of unintentional Fe impurities, $N \sim 10^{15}\,cm^{-3}$, would be sufficient to lead to an A value of $10^7\,s^{-1}$, large enough to adversely impact the efficiency of light-emitting devices.[8] The presence of iron can also affect the performance of electronic devices. For example, current collapse in AlGaN/GaN HEMTs has a strong correlation with Fe doping in the GaN buffer.[4]

Efficient SRH recombination requires high capture rates for both electrons and holes [see Eq. (1)]. Since C_n and C_p decrease approximately exponentially with the energy of the transition,[14] it is generally assumed that only midgap states can lead to an efficient SRH recombination. The behavior of iron as an efficient recombination center is therefore surprising, since it has a deep acceptor level $\sim$0.6 eV from the conduction-band minimum (CBM).[15–17] The position of this level leads to a high electron capture rate, but is so far from the valence-band maximum (VBM) in GaN that the hole capture rate would be negligibly small.

In this Letter, we resolve the puzzle by pointing out the importance of excited states in the recombination cycle. We perform first-principles calculations based on hybrid density functional theory (DFT) that provide detailed information about both ground states and excited states of substitutional Fe in GaN. Such excited states have been experimentally observed in luminescence and absorption studies of GaN:Fe.[16,18] We demonstrate how these excited states lead to efficient electron and hole capture in a cycle that does not even involve the ground state, rendering Fe as an efficient nonradiative recombination center.

Our calculations are based on DFT using the Vienna Ab initio Simulation Package VASP.[19,20] A fraction of screened Fock exchange $\alpha = 0.31$ in the Heyd-Scuseria-Ernzerhof (HSE) hybrid functional[21] leads to an accurate band structure for GaN with a bandgap of 3.48 eV and a reliable description of defect levels.[22] We also performed calculations using the

Random Phase Approximation.[23,24] We used the projector augmented wave (PAW) approach[25] with a plane-wave energy cutoff of 400 eV. Ga *d* states were treated as part of the core. Our tests indicate that including the Ga *d* states as valence states results in transition levels for Fe_{Ga} that differ from *d*-in-the-core by less than 0.02 eV. Point-defect calculations were performed using a 96-atom supercell and the Brillouin zone was sampled at a special *k*-point $k = (1/4, 1/4, 1/4)$. Spin polarization was included in all cases. Spin configurations were calculated by enforcing the spin multiplicity. Tests using a 192-atom supercell showed transition levels changed by less than 0.09 eV. We consider nonradiative capture that occurs via multi-phonon emission.[14] Electron and hole capture coefficients are computed from first-principles following the methodology described in Ref. 26. Calculations of the electron-phonon coupling matrix elements utilized the PAW wave functions within VASP for the valence-band, conduction-band, and defect states.

The formation energy of substitutional Fe on the Ga site in GaN is given by[22]

$$E^f(\mathrm{Fe}^q_{\mathrm{Ga}}) = E_{\mathrm{tot}}(\mathrm{Fe}^q_{\mathrm{Ga}}) - E_{\mathrm{tot}}(\mathrm{GaN}) + \mu_{\mathrm{Ga}} - \mu_{\mathrm{Fe}} + qE_F + \Delta^q, \quad (2)$$

where $E_{tot}(GaN)$ is the total energy of the pristine GaN supercell, $E_{tot}(Fe^{\ q}_{Ga})$ is the total energy of the structure containing the impurity in charge state *q*, and μ_{Ga} and μ_{Fe} are the chemical potentials of Ga and Fe. μ_{Ga} can vary between Ga-rich (equilibrium with bulk Ga) and Ga-poor conditions (equilibrium with N_2 molecules). For μ_{Fe}, the upper limit is set by the solubility-limiting phase, Fe_3N. E_F is the Fermi level, which is referenced to the VBM of GaN, and Δ^q is the finite-size correction for charged defects.[27]

Formation energies for various configurations of iron in GaN are shown in Fig. 1. Iron on the nitrogen site (Fe_N) and in an interstitial configuration (Fe_i) have very high formation energies, larger than the formation energy of Fe_{Ga} regardless of the position of E_F or the choice of chemical potential. Hence, they are unlikely to occur. Indeed, electron paramagnetic resonance (EPR) measurements on the Fe-doped GaN have observed Fe substituting on the Ga site,[28] consistent with our finding that Fe_{Ga} has the lowest formation energy.

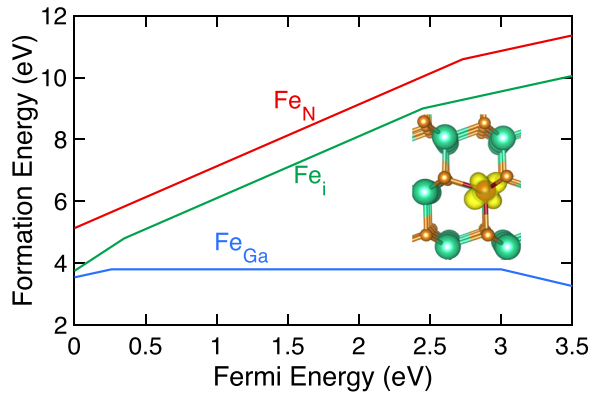

FIG. 1. Formation energy versus Fermi level for Fe_{Ga}, Fe_N and Fe_i in GaN in different charge states, under Ga-rich conditions. The wave function of the defect state of Fe_{Ga} in the negative charge state is illustrated as an inset.

Fe_{Ga} occurs in high-spin configurations. The crystal field splits the 3*d* states into e_g and t_{2g} states (deviations from tetrahedral symmetry in the wurtzite phase are minor), and exchange splits the states into spin-up and spin-down states. The neutral charge state, Fe^0_{Ga}, is a spin sextuplet ($S = 5/2$). This state is commonly referred to as Fe^{3+}, where the "3+" indicates the oxidation state, and we will follow this notation in this Letter. We find the occupied Fe *d* spin-up states to be located just below the GaN valence band, ~7.3 eV below the VBM. The corresponding unoccupied spin-down states are located 0.57 eV above the CBM at Γ. The lattice distortion of the Fe^{3+} state is small, with the four nearest-neighbor N atoms moving outwards by 0.5% of the Ga-N bond length.

The negative charge state, Fe^-_{Ga} (or 2+ oxidation state, Fe^{2+}), is a spin quintuplet ($S = 2$). The four nearest-neighbor N atoms move outwards by 4%. One spin-down *d* state is now occupied, and has moved into the gap; the corresponding wave function is shown in the inset of Fig. 1. Figure 1 shows that the (0/–) (or Fe^{3+}/Fe^{2+}) thermodynamic transition level (acceptor level) is located 0.50 eV below the CBM. This result agrees with previous theoretical calculations[17] and is consistent with transient capacitance measurements[15] and with UV-VIS transmission spectra showing an absorption peak at ~3 eV in Fe-doped GaN.[16]

In the positive charge state, Fe^+_{Ga} (4+ oxidation state), the Fe-N bonds relax inwards by 1.1% of the Ga-N bond length. The (+/0) (or Fe^{4+}/Fe^{3+}) thermodynamic transition level occurs at 0.26 eV above the VBM.

We now calculate the capture coefficients for electron and hole capture for the Fe_{Ga} defect. The location of the (0/–) (Fe^{3+}/Fe^{2+}) level, at 0.5 eV below the CBM, enables fast electron capture by defects in the neutral charge state. However, capturing a hole from the VBM into the negative charge state of Fe_{Ga} (Fe^{2+}) would be a very slow process, since the energy of this transition is 3.0 eV. Our calculated hole capture coefficient for this process is lower than 10^{-20} $cm^3\ s^{-1}$, severely limiting the overall nonradiative recombination rate [Eq. (1)], which is dominated by the *slower* of the two processes. Invoking a *radiative* process for hole capture into the negative charge state of Fe_{Ga} (Fe^{2+}) does not help: capture coefficients associated with band-to-defect transitions in GaN are on the order of 10^{-14} –10^{-13} $cm^3\ s^{-1}$,[29] many orders of magnitude smaller than the values required for efficient SRH recombination.

The consideration of excited states of Fe^{3+} and Fe^{2+} drastically changes the recombination process. Starting from the sextuplet ($S = 5/2$) ground state of Fe^{3+} (corresponding to $^6A_1$), quadruplet ($S = 3/2$) excited states can be obtained by a spin flip. Malguth *et al.*[16] argued that in a tetrahedral crystal field these quadruplet states arise in the order $^4T_1$, $^4T_2$, ^4E, and $^4A_1$ (the latter two being degenerate); although GaN has wurtzite rather than zinc-blende symmetry, we will also adopt this notation here, as is common practice in the literature. A luminescence peak observed at 1.299 eV was attributed to the $^4T_1 \rightarrow {}^6A_1$ transition, and transitions at 2.01 eV and 2.73 eV to two higher-lying excited states were also observed in absorption.[16,18] More recently, Neuschl *et al.*[18] proposed a different ordering of the quadruplet states, namely, $^4T_1$, ^4E, $^4T_2$, and $^4A_1$, without any degeneracy.

In the case of Fe^{2+}, optical spectroscopy also provided evidence for a quintuplet ($S=2$) $^5T_2$ excited state 0.39 eV above the ^5E ground state.[16] In addition, the existence of a triplet excited state is dictated by the C_{3v} symmetry of Fe^{2+},[30] though this state has not yet been experimentally observed in GaN. The $^3T_1$ triplet state *has* been observed for neutral Fe in ZnSe in ZnSe:Fe,[31] which shows luminescence at 1.26 eV corresponding to a transition from this excited state to the ^5E ground state. The similarity between Fe^{2+} in ZnSe and GaN is supported by the observation of the $^5T_2$ excited state in ZnSe at 0.40 eV above the ^5E ground state,[31] very similar to the 0.39 eV difference between the $^5T_2$ and ^5E states of Fe^{2+} in GaN.[16]

In our calculations, we evaluate the excited-state energies of Fe^{3+} and Fe^{2+} from differences in total energy within the Delta-self-consistent-field (ΔSCF) formalism.[32] For the excited state of each charge state we allow for a full relaxation of all internal coordinates. For Fe^{3+} HSE calculations produce $E_0^{q=0}(S=3/2)-E_0^{q=0}(S=5/2)=1.55\,\text{eV}$, where E_0 corresponds to the ground-state energy for a given spin multiplet. ΔSCF calculations using RPA produce a value of 1.40 eV. Both HSE and RPA, thus, slightly overestimate the energy separation between the $^4T_1$ and $^6A_1$ states, which was experimentally determined to be 1.299 eV.[16,18] When applied to Fe^{2+}, HSE calculations find the $^3T_1$ excited state 1.46 eV above the ^5E ground state, again a slight overestimate (by 200 meV) compared to the experimental energy for the corresponding transition (in ZnSe).

Our ΔSCF calculations thus produce very reasonable results for the lowest-energy configurations of a given spin multiplicity. In particular, they confirm that there is indeed a spin-triplet excited state for Fe^{2+}. However, one has to be very cautious in interpreting calculated energies: in order to describe spin multiplet states, one often needs wavefunctions composed of more than one Slater determinant,[33] and this goes beyond the Kohn-Sham picture. For these reasons, in order to describe the energies of the ^4E, $^4T_2$, and $^4A_1$ states of Fe^{3+}, and of the $^5T_2$ state of Fe^{2+}, we rely on the results by Neuschl *et al.*[18] and O'Donnell *et al.*[31] cited above. For consistency, we also take the energies of the $^4T_1$ (for Fe^{3+}) and $^3T_1$ (for Fe^{2+}) states from experiment. A formation energy diagram that includes the excited states is shown in Fig. 2.

The excited states open up new channels for nonradiative capture of electrons and holes. Fig. 3 is an energy level diagram that illustrates the sequence of processes that leads to efficient nonradiative capture of carriers due to the excited states of Fe^{3+} and Fe^{2+}. As noted above, electron capture is a fast process, leading to the ^5E state of Fe^{2+} [Figs. 2 and 3(a)], but hole capture to go back to the $^6A_1$ ground state of Fe^{3+} would be a very slow process. However, as seen in Figs. 2 and 3(b), a transition from the ^5E state to an *excited* state of Fe^{3+} can easily occur; for example, the level for a transition to the $^4T_2$ state is only 0.36 eV above the VBM. Once in the $^4T_2$ state, the system will rapidly lose energy (through spin-conserving intra-defect multiphonon emission) to end up in the $^4T_1$ state, which has the lowest energy among the quadruplet states of Fe^{3+}.

One might think that the next step would be a transition to the $^6A_1$ ground state of Fe^{3+}. However, that transition

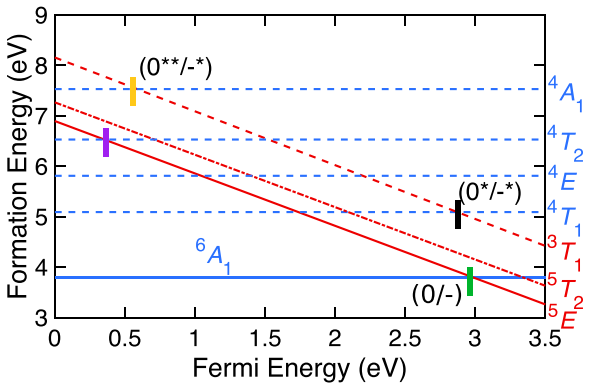

FIG. 2. Formation energy diagram for Fe_{Ga} under Ga-rich conditions. The blue solid line corresponds to the ground state of the neutral ($q=0$) charge state, Fe^{3+}. The blue dashed lines correspond to the quadruplet excited states of Fe^{3+}.[18] The red solid line corresponds to the quintuplet ground state and the dashed-dotted line corresponds to the quintuplet excited state of the negative ($q=-1$) charge state, Fe^{2+}. The red dashed line corresponds to the triplet excited state of Fe^{2+}. The vertical bars indicate transition levels at which hole and electron capture can occur into the ground or excited-state levels. The term symbols for the ground state and excited states are shown along the vertical axis on the right. (0/–) is the thermodynamic transition level of the Fe^{3+}/Fe^{2+} ground state, $(0^*/-^*)$ is the transition level between the $^4T_1$ excited state of Fe^{3+} and the $^3T_1$ excited state of Fe^{2+}, and $(0^{**}/-^*)$ is the transition level between the $^4A_1$ excited state of Fe^{3+} and the $^3T_1$ excited state of Fe^{2+}.

(which gives rise to the characteristic 1.299 eV emission) is spin-forbidden, and as a result, it is very slow, with an 8 ms lifetime.[34] Instead, starting from $^4T_1$, rapid nonradiative electron capture can occur resulting in the $^3T_1$ excited state of Fe^{2+}; this process is indicated with the vertical bar marked $(0^*/-^*)$ in Fig. 2 (at 0.64 eV below the CBM). Transitions from $^3T_1$ to lower-lying states for Fe^{2+} are, again, spin-forbidden, and therefore, it is more likely that this state captures a hole and converts to the $^4A_1$ state. This process is indicated with the vertical bar marked $(0^{**}/-^*)$ (at 0.58 eV above the VBM). From here on, the cycle can rapidly repeat, with the system making transitions between the excited states [Fig. 3(c)].

The conclusion is that nonradiative recombination involves the quadruplet manifold of Fe^{3+} and the triplet excited state of Fe^{2+}. This results in a very efficient nonradiative recombination due to the fast capture of both electrons and holes and spin-conserving nonradiative intra-defect

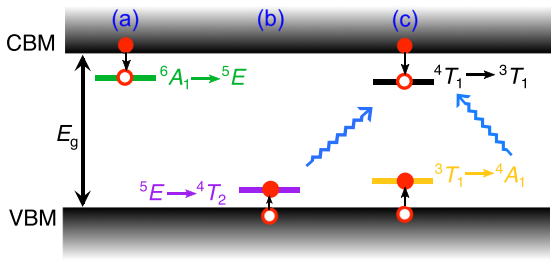

FIG. 3. Nonradiative recombination cycle due to Fe in GaN. (a) Electron capture into the (0/–) level 0.5 eV below the CBM (corresponding to the experimentally observed acceptor level) marked with the green vertical bar in Fig. 2. (b) Hole capture into the level marked with the purple vertical bar in Fig. 2. (c) Once the cycle is initiated, electron and hole capture proceeds between the excited-state transition levels marked by the black $(0^*/-^*)$ and yellow $(0^{**}/-^*)$ vertical bars in Fig. 2. Spin-conserving intra-defect relaxations are illustrated with blue wiggly arrows.

transitions. The calculated capture coefficients, at room temperature, are $C_n = 1.1 \times 10^{-8}$ cm^3 s^{-1} for the $(0^*/-^*)$ transition and $C_p = 7.1 \times 10^{-8}$ cm^3 s^{-1} for the $(0^{**}/-^*)$ transition. These values compare favorably with $C_n = 5.5 \times 10^{-8}$ cm^3 s^{-1} and $C_p = 1.8 \times 10^{-8}$ cm^3 s^{-1} obtained from time-resolved photoluminescence measurements.[13] The agreement is particularly impressive given that these coefficients depend exponentially on transition energies. The calculated C_n value is a bit too small, while C_p is a bit too large. If the energy position of the $^3T_1$ state would shift up by a mere 0.1 eV, both C_n and C_p would be in almost perfect agreement with experiment. The total nonradiative capture coefficient is approximately 10^{-8} cm ^{3}s^{-1}. If we assume the defect density to be 10^{15} cm^{-3} (a very conservative value), the SRH coefficient A [Eq. (1)] is $\sim 10^7$ s^{-1}, a value that can impact the efficiency of optoelectronic devices.[8]

In summary, based on the first-principles calculations and careful analysis of electron and hole capture coefficients, we have evaluated nonradiative recombination rates for Fe impurities in GaN. We have solved the puzzle as to how Fe, which is known to be an acceptor with a level far from midgap ($\sim$0.5 eV below the CBM) can be an efficient SRH center. The critical role of excited states was elucidated.

We gratefully acknowledge the discussion with T. K. Uždavinys. This work was supported by the U.S. Department of Energy (DOE), Office of Science, Basic Energy Sciences (BES) under Award No. DE-SC0010689. The work by A.A. was supported by Marie Sklodowska-Curie Action of the European Union (Project Nitride-SRH, Grant No. 657054). Computational resources were provided by the National Energy Research Scientific Computing Center, which is supported by the DOE Office of Science under Contract No. DE-AC02-05CH11231.

[1]S. Nakamura and M. R. Krames, Proc. IEEE **101**, 2211 (2013).
[2]U. K. Mishra, P. Parikh, and Y.-F. Wu, Proc. IEEE **90**, 1022 (2002).
[3]W. Li, S. Sharmin, H. Ilatikhameneh, R. Rahman, Y. Lu, J. Wang, X. Yan, A. Seabaugh, G. Klimeck, D. Jena, and P. Fay, IEEE J. Explor. Solid-State Comput. Devices Circuits **1**, 28 (2015).
[4]D. Cardwell, A. Sasikumar, A. Arehart, S. Kaun, J. Lu, S. Keller, J. Speck, U. Mishra, S. Ringel, and J. Pelz, Appl. Phys. Lett. **102**, 193509 (2013).
[5]P. Alippi, F. Filippone, G. Mattioli, A. A. Bonapasta, and V. Fiorentini, Phys. Rev. B **84**, 033201 (2011).
[6]J. Baur, K. Maier, M. Kunzer, U. Kaufmann, J. Schneider, H. Amano, I. Akasaki, T. Detchprohm, and K. Hiramatsu, Appl. Phys. Lett. **64**, 857 (1994).
[7]A. Istratov and E. Weber, Appl. Phys. A **66**, 123 (1998).
[8]A. David and M. J. Grundmann, Appl. Phys. Lett. **96**, 103504 (2010).
[9]S. Mookerjea, D. Mohata, T. Mayer, V. Narayanan, and S. Datta, IEEE Electron Device Lett. **31**, 564 (2010).
[10]W. Shockley and W. Read, Jr., Phys. Rev. **87**, 835 (1952).
[11]R. N. Hall, Phys. Rev. **87**, 387 (1952).
[12]T. Aggerstam, A. Pinos, S. Marcinkevičius, M. Linnarsson, and S. Lourdudoss, J. Electron. Mater. **36**, 1621 (2007).
[13]T. K. Uždavinys, S. Marcinkevičius, J. H. Leach, K. R. Evans, and D. C. Look, J. Appl. Phys. **119**, 215706 (2016).
[14]C. H. Henry and D. V. Lang, Phys. Rev. B **15**, 989 (1977).
[15]A. Polyakov, N. Smirnov, A. Govorkov, N. Pashkova, A. Shlensky, S. Pearton, M. Overberg, C. Abernathy, J. Zavada, and R. Wilson, J. Appl. Phys. **93**, 5388 (2003).
[16]E. Malguth, A. Hoffmann, and M. R. Phillips, Phys. Status Solidi B **245**, 455 (2008).
[17]Y. Puzyrev, R. Schrimpf, D. Fleetwood, and S. Pantelides, Appl. Phys. Lett. **106**, 053505 (2015).
[18]B. Neuschl, M. Gödecke, K. Thonke, F. Lipski, M. Klein, F. Scholz, and M. Feneberg, J. Appl. Phys. **118**, 215705 (2015).
[19]G. Kresse and J. Hafner, Phys. Rev. B **47**, 558 (1993).
[20]G. Kresse and J. Furthmüller, Phys. Rev. B **54**, 11169 (1996).
[21]J. Heyd, G. E. Scuseria, and M. Ernzerhof, J. Chem. Phys. **118**, 8207 (2003).
[22]C. Freysoldt, B. Grabowski, T. Hickel, J. Neugebauer, G. Kresse, A. Janotti, and C. G. Van de Walle, Rev. Mod. Phys. **86**, 253 (2014).
[23]M. Kaltak, J. Klimeš, and G. Kresse, J. Chem. Theory Comput. **10**, 2498 (2014).
[24]M. Kaltak, J. Klimeš, and G. Kresse, Phys. Rev. B **90**, 054115 (2014).
[25]P. E. Blöchl, Phys. Rev. B **50**, 17953 (1994).
[26]A. Alkauskas, Q. Yan, and C. G. Van de Walle, Phys. Rev. B **90**, 075202 (2014).
[27]C. Freysoldt, J. Neugebauer, and C. G. Van de Walle, Phys. Status Solidi B **248**, 1067 (2011).
[28]J. Dashdorj, M. Zvanut, J. Harrison, K. Udwary, and T. Paskova, J. Appl. Phys. **112**, 013712 (2012).
[29]M. A. Reshchikov, AIP Conf. Proc. **1583**, 127 (2014).
[30]B. Henderson and G. F. Imbusch, *Optical Spectroscopy of Inorganic Solids* (Oxford University Press, 2006), Vol. 44.
[31]K. O'Donnell, K. Lee, and G. Watkins, J. Phys. C.: Solid State Phys. **16**, L723 (1983).
[32]R. O. Jones and O. Gunnarsson, Rev. Mod. Phys. **61**, 689 (1989).
[33]U. von Barth, Phys. Rev. A **20**, 1693 (1979).
[34]R. Heitz, P. Thurian, I. Loa, L. Eckey, A. Hoffmann, I. Broser, K. Pressel, B. Meyer, and E. Mokhov, Appl. Phys. Lett. **67**, 2822 (1995).